

Stripping Voltammetric, Conductance and Anodic Linear Polarization Analysis on Dissolution of Electrodeposited Zinc-Cobalt Alloy

M. M. Abou-krisha^{1,*} and A. M. Abushoffa²

¹Chemistry Department, Faculty of Science, South Valley University, Qena, Egypt.

²Department Pharmaceutical Chemistry, Faculty of Pharmacy, Al-Fateh University Tripoli, Libya.

*E-mail: mortaga_aboukrisha@yahoo.com

Received: 28 March 2007 / Accepted: 11 April 2007 / Published: 1 May 2007

The electrodeposition of zinc-cobalt alloys from sulfate bath was studied on steel substrate. In order to elucidate the deposition mechanism a complementary approach was used based on the combination of various electrochemical techniques. Under the studied experimental conditions, the electrodeposition of the alloys was of anomalous type. The dissolution rate of electrodeposited Zn-Co, from sulfate bath, in hydrochloric acid was investigated. Two techniques, the stripping voltammetry and the conductance measurements, were used for the first time in this concern. The anodic linear polarization measurements used to study the dissolution process and to confirm the others techniques results. A comparison was carried out between those newly suggested methods and the previously used method. This comparison shows of the reliability of these methods. X-ray diffraction measurements revealed that the alloy consisted of the two kinds of deposits have been formed, pure Zn and γ -phase ($\text{Co}_5\text{Zn}_{21}$). The comparison between Co deposition and Zn-Co codeposition showed that the remarkable inhibition of Co deposition takes place due to the presence of Zn^{2+} in the plating bath. The Co deposition starts at -0.87 V in the bath of Co deposition only, but its deposition starts at more negative potentials in the codeposition bath although the concentration of Co^{2+} is the same in the both baths.

Keywords: Zn-Co alloy; dissolution rate; stripping voltammetry; anodic linear polarization; anomalous codeposition

1. INTRODUCTION

Electroplated zinc coatings on steel substrate are considered as one main way for the corrosion protection of steel. Recently, the interest of Zn-Ni and Zn-Co alloy coatings has increased owing to their better mechanical and corrosion properties compared with pure zinc coatings [1-8]. For corrosion protection, the alloy needs a low surface area with either a high content of Zn, which is less noble than steel (sacrificial film) or a high content of Co, which is more noble than steel (barrier film).

Developing and studying electrolytes, from which Zn alloys are electrodeposited, is a high-priority problem in electroplating. The use of zinc and its alloys for improving the dissolution resistance of coated steel, has been growing worldwide [9-11] and as a substitute for toxic and high-cost cadmium coatings [12]. In the automotive industry, for example, its use has been growing in search of increasing the dissolution resistance of chassis six times superior to that obtained with pure zinc deposits [13]. Many studies have attempted to understand the characteristics of the deposition process of Zn alloys [2,14]. The electrodeposition of Zn-Co alloys is classified by Brenner [15] as an anomalous codeposition where zinc, the less noble metal, is preferentially deposited. Although this phenomenon [15] has been known since 1907, the codeposition mechanisms of zinc alloys are not well understood. There are some propositions to explain the anomalous codeposition of the Zn-Co alloys. The first attributes the anomalous codeposition to a local pH increase, which would induce zinc hydroxide precipitation and would inhibit the cobalt deposition [14]. Another proposition is based on the underpotential deposition of zinc on nickel (or cobalt)-rich zinc alloys or on nickel (or cobalt) nuclei [16-17].

Two other propositions [14,18] on NiFe electrodeposition propose different mechanisms. The first mechanism [14] assumes that Ni^{2+} discharges first to form a thin layer which chemisorbs water to form adsorbed $\text{Ni}(\text{OH})^+$. Competition between the Ni^{2+} and Fe^{2+} to occupy active sites leads to the preferential deposition of Fe. Matlosz [18] uses a two-step reaction mechanism involving adsorbed monovalent intermediate ions for both electrodeposition of iron and nickel, as single metals, and combines the two to develop a model for codeposition. Anomalous effects assumed to be caused by preferential surface coverage due to differences in Tafel rate constants for electrodeposition.

Sasaki and Talbot [19] proposed a model which extends the one-dimensional diffusion modeling of Grande and Talbot [20], a supportive or interpretive, rather than a predictive, model of electrodeposition. A main contribution of this model is the inclusion of hydrogen adsorption and its effects on electrodeposition. N. Zech et. al. [21] have concluded that codeposition of iron group metals leads to a reduction of the reaction rate of the more noble component and an increase of the reaction rate of the less noble component compared to single metal deposition.

Many techniques were suggested to investigate the dissolution of Zn alloys in different media [22-23]. In the present work, the dissolution of Zn-Co alloy in HCl was examined using stripping voltammetry [24-26] conductance [24,25,27] and anodic linear polarization techniques [22-23]. The stripping voltammetry which is capable of detecting and determining very small amounts of cations is applied for the first time to follow up the minute traces of Zn^{2+} [26,28] and Co^{2+} [28] in HCl. Conductance measurement technique is chosen to study the dissolution rate, since the conductivity decreases attributed to the decrease in the concentration of H^+ which involved during the alloy dissolution in HCl and can be easily detected by conductometer.

The aim of this work is to investigate the mechanism of Zn-Co alloy deposition in sulfate electrolytes. The results of the experimental approach, based essentially on the analysis of the deposit compositions, and the cyclic voltammograms and galvanostatic measurements during the electroplating. Concerning the dissolution study, the stripping voltammetry and the conductance measurements were used. The dissolution behavior of the deposits was also investigated using anodic linear polarization resistance.

2. EXPERIMENTAL PART

The electrolytes used for electrodeposition of Zn-Co alloy were freshly prepared using Analar grade chemicals without further purification and doubly distilled water. The composition of the standard bath was 0.20 M ZnSO₄, 0.20 M CoSO₄, 0.20 M H₃BO₃, 0.01 M H₂SO₄, and 0.20 M Na₂SO₄, and the pH was adjusted at 2.5.

For electrodeposition of Zn and Co metals and their alloys, a steel sheet (for conductance measurements and stripping voltammetry), steel rod (for galvanostatic measurements, cyclic voltammetry and anodic linear polarization), and stainless steel sheet (for chemical composition) cathodes and platinum anodes were used. Galvanostatic measurements[10], cyclic voltammetry[10] and anodic linear polarization were carried out with an EG&G potentiostat/galvanostat Model 237A controlled by a PC using 352 corrosion software and the experiments have been done without cathode movement or solution agitation. The specimens of steel sheets (99.98%Purity) were of dimensions of 0.05 cm in thickness, 2.0 cm in width and 3.0 cm in length. 304-stainless steel sheets were of dimensions of 0.05 cm in thickness, 1.0 cm in width and 1.0 cm in length. Steel and stainless steel sheets provided with a narrow strip of about 1 cm² area to which clamp terminals were attached for electrical contact. Pure steel rod was in a Teflon mount so that only its cross-sectional area (0.196 cm²) was in contact with solution. Platinum anode of large area (6.0 cm²) was used as a counter electrode. A conventional electrochemical cell of 100.0 cm³ capacity was used for the present work [10].

The cathode coated with parent metals or Zn-Co was removed, washed then dissolved and analyzed. The chemical composition of parent metals of Zn-Co electrodeposits were determined using Atomic Absorption Spectroscopy (Variian spectrAA 55). The Zn and Co content in the deposit were confirmed by EDS (Energy Dispersive X-ray Spectrometer) system with link Isis[®] software and model 6587 X-ray detector (OXFORD, England). Using the resultant analysis, the film thickness and the cathode current efficiency of the deposit from the selected baths on steel were calculated. The thickness of the deposited alloy layer is approximately estimated from the amount of deposit and the densities of Zn ($d_{Zn} = 7.14 \text{ g cm}^{-3}$) and Co ($d_{Co} = 8.90 \text{ g cm}^{-3}$) of the same surface area [2].

The dissolution resistance behavior of the coated steel by Zn-Co alloy, using galvanostatic technique, under different conditions was studied using stripping voltammetry, conductance measurements and linear polarization technique.

A computer-aided electrochemistry system was used in the voltammetric studies. The system consists of the following: -

- i- A potentiostat model 263 (EG & PARC) princeton applied research corporation (made in USA).
- ii- A static mercury drop electrode (SMDE) model 303A PARC.
- iii- A 305 magnetic stirrer PARC.
- iv- Electroanalytical software models 270/250 version 4.0 (PARC) which controls the potentiostat via IEEE 488 GPIB.

The stripping voltammetric measurements were carried out by placing 100 cm³ of 0.20 M HCl in a 100 cm³ beaker and thermostated at the working temperature. The cleaned alloy specimen was then immersed vertically in the solution and the time started. Changes in the concentration of Zn²⁺

and/or Co^{2+} were followed by withdrawing 0.10 cm^3 of the solution each time, completed to 100.0 cm^3 by the reagent solution, using the procedures previously conducted by M. M. Ghoneim et. al.[28], and the current corresponding to the concentration of ions was recorded. The concentration of ions was calculated from standard working curves.

It is interesting to mention that the composition of the deposited alloy can be detected also (to confirm that detected by Atomic Absorption Spectroscopy) from the measured concentrations using stripping analysis when it becomes constant with time.

Conductance measurements technique is chosen to study the dissolution behavior of parent metals and Zn-Co alloys plated on steel sheets, detected by conductivity Meter Model 4320. To carry out conductance measurements, 100 cm^3 of 0.2 M HCl was placed in a beaker with constant continuous stirring at 30.0°C using air thermostat. Then the plated steel sheets specimen was immersed vertically in the solution and the change of conductance of HCl were recorded at different time intervals. The first look at the K-t curves shows a distinct decrease of conductance with time at first portion then passing through a constant conductance after dissolution of the deposit. The linear character or semi steady state is mainly attributed to the beginning of the dissolution of steel which possesses highly dissolution resistance in HCl.

It is important to say that the more time (t_c) taken to reach the semi steady state the more dissolution resistance. Where, (t_c), is the time required to dissolve the deposit and directly proportional to the dissolution resistance of the deposit. The value of $1/t_c$ can be considered as a function of the dissolution rate of the deposit [27].

To measure the dissolution resistance of the deposit, the linear polarization technique was used. In this technique the steel-coated galvanostatically by Zn-Co alloy was washed and transferred into the electrolytic cell containing 100 cm^3 0.02 M HCl in order to anodically dissolve the coating. The anodic dissolution of deposits in a voltammetric mode was conducted at a potential scan rate of 2 mV s^{-1} . The values of electrochemical corrosion measurements of the coatings, E_{corr} - corrosion potential, I_{corr} - corrosion current, R_p - polarization resistance and corrosion rate, were obtained and represented in Table 3.

All experiments were duplicated and the reproducibility for this type of measurements was found to be satisfactory.

3. RESULTS AND DISCUSSION

3.1. Treatment of the data

3.1.1. Data from stripping voltammetry

Results of the variation of Zn^{2+} (Figure 1a) and Co^{2+} (Figure 1b) concentrations accumulated in HCl during the dissolution of the deposited Zn-Co with time are represented in Figure 1. The correlation and regression coefficients for Zn dissolution from the deposit Zn-Co (as an example) are reported in Table (1). It was found that Zn^{2+} and Co^{2+} concentrations increased continuously with time and then constant after the whole deposited dissolve.

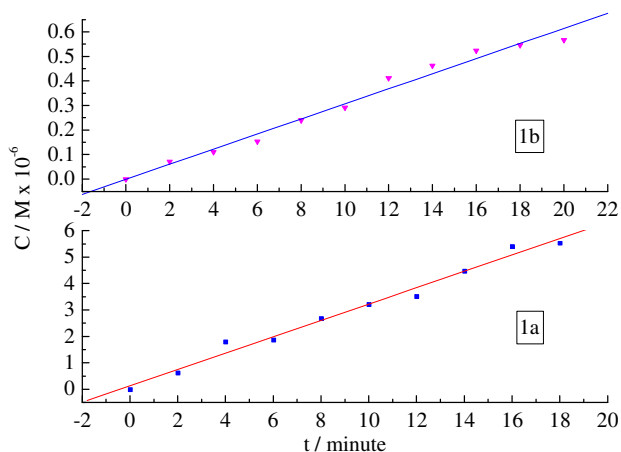


Figure 1. C-t curves for the dissolution of the deposit Zn-Co [(1a) for Zn] and [(1b) for Co] on steel (12 cm²), plated from a bath containing 0.20 M ZnSO₄, 0.20 M CoSO₄, 0.01 M H₂SO₄, 0.20 M Na₂SO₄ and 0.20 M H₃BO₃ at 10 mA cm⁻² for 10 minutes at 30.0°C, in 100 cm³ 0.20 M HCl at 30.0°C.

Table 1. The regression data for the dissolution of Zn from the deposit Zn-Co on steel (12 cm²), plated from a bath containing 0.20 M ZnSO₄, 0.20 M CoSO₄, 0.01 M H₂SO₄, 0.20 M Na₂SO₄ and 0.20 M H₃BO₃ at 10 mA cm⁻² for 10 minutes at 30.0°C, in 100 cm³ 0.20 M HCl at 30.0°C.

Linear regression	eq. $y=A+Bx$ i.e $c = A + B \tau$	
	B	3.097E-7
	r	0.993
Power regression	eq. $y=A x^B$ i.e $c = A \tau^B$ or $\ln c = \ln A + B \ln \tau$	
	B	0.7554
	r	0.989
Exponential regression	eq. $y=A e^{Bx}$ i.e $c = A e^{B\tau}$ or $\ln c = \ln A + B \tau$	
	B	0.1171
	r	0.930
Logarithmic regression	eq. $y=A + B \ln x$ i.e $c = A + B \ln \tau$	
	B	2.282E-8
	r	0.937
$v, \text{mg cm}^{-2} \text{min}^{-1}$	1.684E-4	

The correlation, between the concentration C and the time τ , can expressed statistically [27] by the following formula:

(i) Linear regression: $C = A' + B' \tau$ (1)

(ii) Logarithmic regression: $C = \dot{A} + \dot{B} \ln \tau$ (2)

(iii) Power regression: $C = A'' \tau^{B''}$ (3)

(iv) Exponential regression: $C = A'^* e^{B'^* \tau}$ (4)

The interpretation of the constants are explained as following:

The first relation shows the linear relationship, where A' is denoted to the concentration of Zn^{2+} or Co^{2+} at $\tau=0$ whereas B' is the concentration of Zn^{2+} or Co^{2+} per minute during the linear relation (i.e. the dissolution rate of Zn or Co expressed in $mol\ dm^{-3}\ min^{-1}$).

In the formula (2) \dot{A} is the concentration of Zn^{2+} or Co^{2+} after one minute. The meaning of the constant \dot{B} was interpreted by using $\tau = e = 2.718281828$ minutes, hence the formula (2) becomes

$$C_{at(\tau=e)} = \dot{A}_{(the\ concentration\ at\ \tau=1)} + \dot{B} \ln e$$

$$\dot{B} = C_{at(\tau=e)} - \dot{A}_{(the\ concentration\ at\ \tau=1)}$$

i.e. B is the concentration of Zn^{2+} or Co^{2+} after e minutes subtracted from its value at one minute.

For the power regression (Formula 3) is became

$$\ln C = \ln A'' + B'' \ln \tau$$

at $\tau = 1$, then $C = A''$

i.e. A'' is the concentration of Zn^{2+} or Co^{2+} at $\tau = 1$, and at $\tau = e$ the formula becomes:

$$\ln C_{at(\tau=e)} = \ln A'' + B''$$

$$B'' = \ln \frac{C_{at(\tau=e)}}{A''}, \text{ if } Z = \text{natural antilogarithm, then}$$

$$Z = \frac{C}{A''}$$

$$C_{at(\tau=e)} = Z A''_{(the\ concentration\ at\ \tau=1)}$$

$$b'' = C_{\tau=e} - A''_{\tau=1} = Z A''_{\tau=1} - A''_{\tau=1}$$

i.e. b'' is the concentration of Zn^{2+} or Co^{2+} after e minutes subtracted from its value at one minute.

The meaning of the constants for the last formula are interpreted by the following:

$$\ln C = \ln A'^* + B'^* \tau$$

It is clear that at $\tau=0$, $C = A'^* =$ (the concentration of Zn^{2+} or Co^{2+} at $\tau=0$), and at $\tau=1$, the formula becomes:

$$\ln C_{at(\tau=1)} = \ln A'^* + B'^*$$

$$B'^* = \ln \frac{C_{at(\tau=1)}}{A'^*}, \text{ if } M = \text{natural antilogarithms, then}$$

$$M = \frac{C}{A'^*}$$

$$C_{at(\tau=1)} = M A'^* \text{ (the concentration at } \tau=0)$$

$$b'^* = C_{\tau=1} - A_{\tau=0} = M A_{\tau=0} - A_{\tau=0}$$

i.e. b'^* is the concentration of Zn^{2+} or Co^{2+} after one minute subtracted from its value at time equal zero.

The dissolution rates (v) of Zn or Co expressed in $mg\ cm^{-2}\ min^{-1}$ were computed {using the relation (5)} from the values of the slop B (the dissolution rate of Zn^{2+} or Co^{2+} expressed in $mol\ dm^{-3}\ min^{-1}$), the regression coefficient for the most fitting relation, namely the linear one, and reported in the same Table 1.

The correlation between C , the concentration of Zn^{2+} or Co^{2+} and τ , the time showed that a linear regression is the best to this relation ($r > 0.99$). Thus Zn^{2+} or Co^{2+} concentration in solution is related to time best of all in the form:

$$C = A' + B' \tau \quad (1)$$

$$v [mg\ Zn\ or\ Co\ (cm^2\ min)^{-1}] = B' [mol\ Zn^{2+}\ or\ Co^{2+}\ (dm^3\ min)^{-1}] \\ \times 100\ cm^3 [1\ dm^3\ (1000\ cm^3)^{-1}] \\ \times [atomic\ weight\ g\ of\ Zn\ or\ Co\ (1\ mol\ Zn^{2+}\ or\ Co^{2+})^{-1}] \\ \times [1(A\ cm^2)^{-1}][1000\ mg\ (1g)^{-1}] \quad (5)$$

where A is the surface area of the deposit (i.e. the surface area of the working electrode).

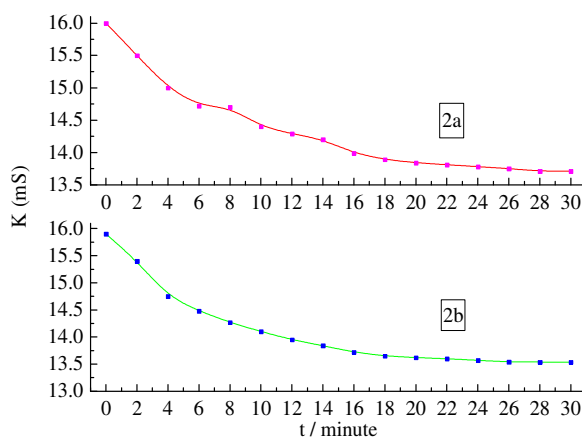


Figure 2. K-t curves [(2a) one curve from first series and (2b) one curve from second series] for the dissolution of the deposit Zn-Co on steel ($12\ cm^2$), plated from a bath containing 0.20 M $ZnSO_4$, 0.20 M $CoSO_4$, 0.01 M H_2SO_4 , 0.20 M Na_2SO_4 and 0.20 M H_3BO_3 at $10\ mA\ cm^{-2}$ for 10 minutes at $30.0^\circ C$, in $100\ cm^3$ 0.20 M HCl at $30.0^\circ C$.

3.1.2. Data from conductance measurements

To verify [29] the reliability of the newly suggested conductance method, two series measurements of steel electrodeposited by Zn-Co (Figure 2 as a representative curves) alloy type, and both series were compared within each type.

Table 2. Values of a, s, s/a, s_{a1-a2} , and t_{a1-a2} of the two series obtained from statistical treatment of $1/t_c$ obtained from the dissolution of deposited Zn-Co on steel (12 cm^2), plated from a bath containing 0.20 M ZnSO_4 , 0.20 M CoSO_4 , 0.01 M H_2SO_4 , 0.20 M Na_2SO_4 and 0.20 M H_3BO_3 at 10 mA cm^{-2} for 10 minutes at 30.0°C , in 100 cm^3 0.20 M HCl at 30.0°C .

No.	$1/t_c$	
	First series	Second series
1	0.06017	0.05875
2	0.06242	0.06053
3	0.06090	0.06017
4	0.05981	0.06127
5	0.06127	0.06402
6	0.06281	0.06090
7	0.05875	0.06053
8	0.06402	0.06361
9	0.06053	0.06053
10	0.05910	0.06242
	$a_1 = 0.06098$	$a_2 = 0.06128$
	$s_1 = 0.00168$	$s_2 = 0.00162$
	$s_1/a_1=0.02755$ $\% = 2.755\%$	$s_2/a_2=0.02644$ $\% = 2.6436\%$
	$a_2 - a_1 = 0.0003$	
	$s_{(a1-a2)} = 0.002333$	
	$\therefore (a_2 - a_1) < s_{(a1-a2)}$	
	$t_{(a1-a2)} = 0.40582$	

Table 2 gives the results of statistical treatment for first and second series of electrodeposited steel respectively. In this Table the values of a (the mean), s (standard deviation), s/a (the coefficient of variation), $s_{(a1-a2)}$ (the difference of the standard deviation) and $t_{(a1-a2)}$ (student criterion). $s_{(a1-a2)}$ and $t_{(a1-a2)}$ are determined as follows:

$$s_{(a1-a2)} = [(s_{a1})^2 + (s_{a2})^2]^{1/2}$$

$$t_{(a1-a2)} = [(a_1-a_2)/ s_{(a1+a2)}] [n_1n_2/(n_1+n_2)]^{1/2}$$

where $s_{(a1+a2)} = \{[\sum(x_1 - a_1)^2 + \sum(x_2 - a_2)^2]/[n_1 + n_2 - 2]\}^{1/2}$

where n_1 and n_2 are the number of experiments with the means a_1 and a_2 respectively. $s_{(a1+a2)}$ is the standard deviation of the combined experimental results, where x_1 and x_2 represent the individual

experimental results of the first and second series. From these it is obvious that the two means are considered to be consistent (i.e., satisfactory agreement), because the difference between the means is less than the standard deviation of the difference. Also, the value of the calculated $t_{(a1-a2)}$ is less than the tabulated t [29], so these results suggest the reliability of the newly suggested conductance method. This technique proved to be sufficiently accurate, sensitive and easy to perform.

3.2. Comparison between deposited Zn, Co, and Zn-Co codeposited

In Figure 3, cyclic voltammograms behaviour of steel at 30.0°C in the bath solutions were represented. Potentiodynamic cathodic polarization measurements (the cathodic part in the cyclic voltammograms) of steel in bath solution in presence of Zn^{2+} or Co^{2+} alone and $Zn^{2+} + Co^{2+}$ together were represented in the same Figure 3. From this Figure it is observed that the deposition of Zn starts at about -1.096 V which takes the same shape and close to the potential of Zn-Co codeposition (about -1.059 V). On the other hand, from the same Figure it is obvious that the Co deposition starts at about -0.87 V and the growth of deposited layer increases gradually when the potential shifts to more negative values. Also, the polarization curve of the alloy deposition lies between the polarization curves of each deposition Zn and Co.

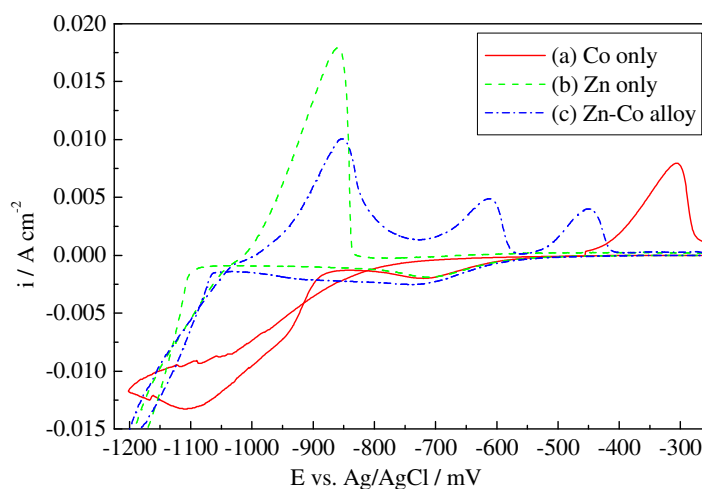


Figure 3. i - E curves (cyclic voltammograms) for steel (0.196 cm^2) in 0.20 M ZnSO_4 (b and c), 0.20 M CoSO_4 (a and c), $0.01 \text{ M H}_2\text{SO}_4$, $0.20 \text{ M Na}_2\text{SO}_4$ and $0.20 \text{ M H}_3\text{BO}_3$ and scan rate 5 mV s^{-1} at 30.0°C .

This position suggested that the codeposition enable Zn to deposit at more positive potential (i.e. shifts the deposition potential of Zn to less negative values) and increase that of Co to more negative ones, due to the presence of Co^{2+} which facilitates Zn deposition. The cathodic peak started at about -0.5 V may be due to the hydrogen evolution, which increase as the pH of the bath decrease. This peak is similar to that appears in absence of both Zn^{2+} and Co^{2+} , so this peak probably appears mainly due to the presence of H_2SO_4 [2]. In the presence of Zn^{2+} and/or Co^{2+} , this cathodic peak was decreased, due to the surface effect occurs with the addition of Zn^{2+} and/or Co^{2+} . This is ascribed to that the addition of Zn^{2+} and/or Co^{2+} (especially Co^{2+}) decreases the adsorption of H^+ and consequently hydrogen

evolution. This may be attributed to start the competitive adsorption between Zn^{2+} and/or Co^{2+} (or its monovalent intermediate) and H^+ [2].

It is appear from the anodic part in the cyclic voltammograms that only one anodic peak at about -0.86 V. This anodic peak corresponds to the anodic dissolution of Zn deposited alone in the absence of Co. Whereas three oxidation peaks were observed for Zn-Co alloy deposit, the first two corresponding to the more negative potentials are attributable to the zinc oxidation in the alloy and the more positive one to the oxidation of the remaining porous cobalt matrix of the alloy. Under this condition, two kinds of deposits have been formed and confirmed by XRD (Figure 4), pure Zn the first dissolution anodic peak] and γ -phase [$(\text{Co}_5\text{Zn}_{21})$ the second dissolution anodic peak]. The third peak corresponding to the dissolution of Co from γ -phase. The behaviour of the layer growth of the Zn deposition in the cathodic direction is seems to be similar to that of the Zn-Co codeposition. Taking into our consideration that the potential of the anodic dissolution of the pure Zn is more positive than that of the Zn deposited alone, the dissolution of the pure Zn in the positive direction is relatively close to that of Zn deposit alone. This can be understood from the fact that the Zn-Co deposit is mainly contained Zn. The Zn-Co codeposition started at about -1.059 V and there is no Co cathodic peak at -0.87 V as mentioned before. The reason for this behavior is ascribed to the presence of Zn^{2+} , which inhibits Co^{2+} electrodeposition.

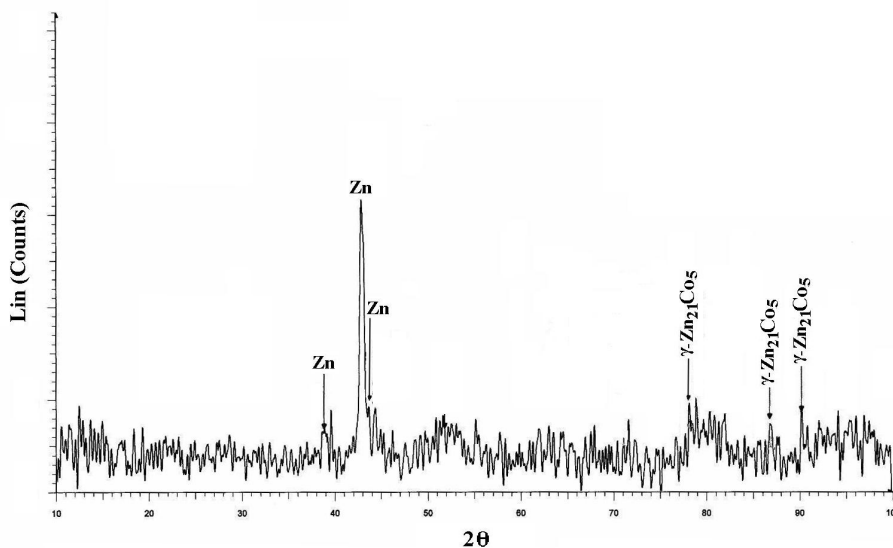


Figure 4. X-ray diffractogram of Zn-Co alloy, deposited on steel (0.196 cm^2) in 0.20 M ZnSO_4 , 0.50 M CoSO_4 , 0.20 M NiSO_4 , $0.01 \text{ M H}_2\text{SO}_4$, $0.20 \text{ M Na}_2\text{SO}_4$ and $0.20 \text{ M H}_3\text{BO}_3$ at 10 mA cm^{-2} for 10 minutes at 30.0°C .

In Zn-Co codeposition both the deposited layer does not grow at the potential -1.059 V (the cathodic current decays with potential as seen in Figure 3) which corresponds to high overvoltage for the Co deposition. Also, in Zn electrodeposition, the cathodic current peak decays with potential after the initial spike means that the nucleus growth of the Zn deposition is probably not induced at the potential of about -1.059 V. In the Co deposition bath in absence of Zn^{2+} , however, the nucleus growth of Co deposition (the cathodic peak increases gradually with potential as seen in Figure 3) is induced at

the smaller overvoltage than the above potential. This means that the adsorbed Zn^{2+} (or its monovalent intermediate) inhibits the nucleus growth of the Co deposition in the Zn-Co codeposition bath.

It is interesting to mention that the height of the anodic peak (The peak current) of the deposited Zn dissolution was higher than that in the case of the codeposited Zn-Co alloy dissolution. This means that the amount of Zn in the alloy less than that in a single metal deposit and gives an indication to the formation of Co in the alloy deposited.

Figure 5 shows the potential-time dependence for the deposition of Zn, Co and Zn-Co alloy on steel at 10 mA cm^{-2} for 10 minutes. It is clear that the deposition of Co needs low overpotential to create the initial nucleus and the deposit grow at low potentials. The deposition of Zn takes place with higher nucleation overpotential and grows at high potential. The Zn-Co codeposited at moderate overpotential; this is due to the deposition of Co is strongly inhibited by the presence of Zn^{2+} , while the deposition of Zn is induced by the presence of Co^{2+} .

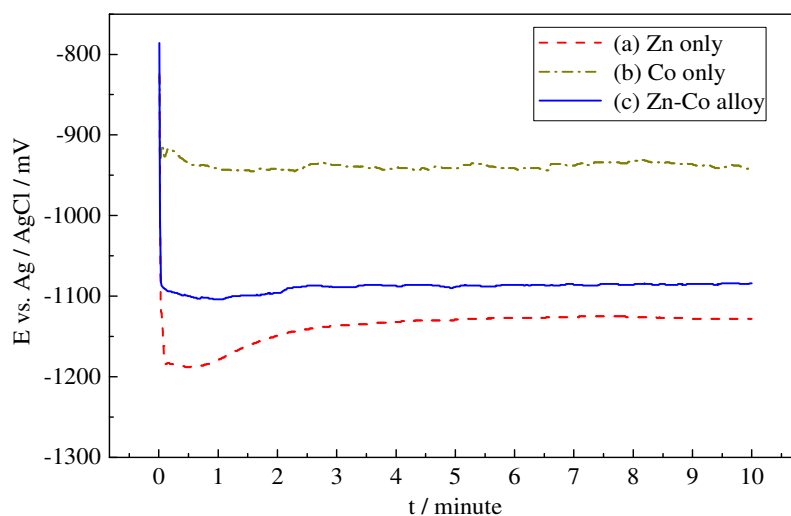


Figure 5. E-t curves for steel (0.196 cm^2) in 0.20 M ZnSO_4 (b and c), 0.20 M CoSO_4 (a and c), $0.01 \text{ M H}_2\text{SO}_4$, $0.20 \text{ M Na}_2\text{SO}_4$ and $0.20 \text{ M H}_3\text{BO}_3$ at 10 mA cm^{-2} for 10 minutes at 30.0°C .

Linear polarization tests (Figure 6) were done using a steel-coated galvanostatically by pure Zn and Co and Zn-Co alloy. From the measured corrosion potential (E_{corr}) listed in Table 3, it is found that the anodic peak of the alloy lies at more positive potential than that of plated Zn alone, this indicate that the plated Zn-Co have higher resistance relative to plated Zn only. It is appear also, that the corrosion rate and current were decreased with the presence of Co in the deposit, but the polarization resistance increased. Thus, the improvement achieved in the corrosion resistance of the alloy deposits can explained by the presence of Co.

The variation of electric conductance with time as a result of dissolution of steel and plated steel by pure Zn and Co and Zn-Co alloy (Figure 7) in the presence of HCl was measured as described in the experimental part. It is observed that the t_c value (Table 3) for plated $\text{Co} > \text{Zn-Co} > \text{Zn}$ and vice versa $1/t_c$ (the dissolution rate) for plated $\text{Co} < \text{Zn-Co} < \text{Zn}$. This means that the Co increases the dissolution resistance of the deposit, but not more than plated pure Co (i.e. anomalous codeposition).

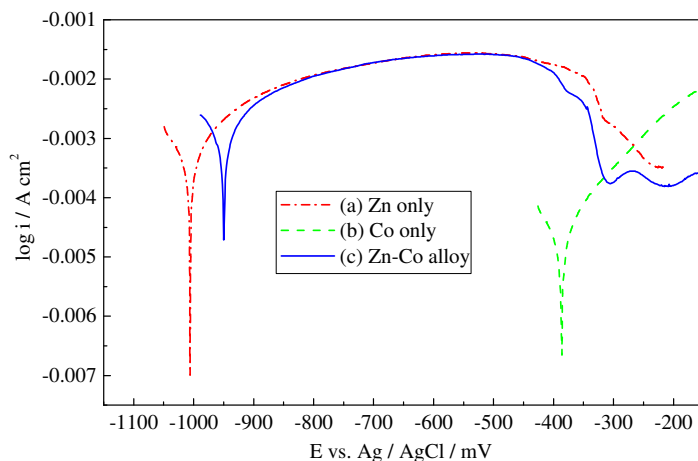


Figure 6. log i - E curves for the dissolution of the deposit Zn-Co on steel (0.196 cm^2), plated from a bath containing 0.20 M ZnSO_4 (a and c), 0.20 M CoSO_4 (b and c), $0.01 \text{ M H}_2\text{SO}_4$, $0.20 \text{ M Na}_2\text{SO}_4$ and $0.20 \text{ M H}_3\text{BO}_3$ at 10 mA cm^{-2} for 10 minutes at 30.0°C , in 100 cm^3 0.02 M HCl at 30.0°C .

Table 3. Values of electrochemical corrosion measurements of the deposit on steel (0.196 cm^2), plated from a bath containing, 0.20 M ZnSO_4 (b and c), 0.20 M CoSO_4 (a and c), $0.01 \text{ M H}_2\text{SO}_4$, $0.20 \text{ M Na}_2\text{SO}_4$ and $0.20 \text{ M H}_3\text{BO}_3$ at 10 mA cm^{-2} for 10 minutes at 30.0°C .

Deposit Parameter	(a) Zn only	(b) Co only	(c) Zn-Co alloy
Zn amount in the deposit / 10^{-5} g	68	0	61.32
Co amount in the deposit / 10^{-5} g	0	38.4	5.45
Total mass of the deposit / 10^{-5} g	68	38.4	66.77
Zn Current efficiency (e_{Zn}) / %	84.83	0	76.65
Co Current efficiency (e_{Co}) / %	0	98.1	15.18
Zn-Co deposit Current efficiency ($e_{\text{Zn-Co}}$) / %	0	0	92.13
Thickness of the deposit / μm	4.84	2.2	4.68
R_p / K-Ohms	1.33	5.34	1.535
$i_{\text{corr.}}$ / $\text{A cm}^{-2} \times 10^{-3}$	3.8	0.26	3.453
Corr. Rate / milli-inches year-1	8987	186.2	8823
($E_{\text{corr.}}$) Corrosion potential / mV	-1011	-489	-1008
t_c	16.33	19.7	16.67
$1/t_c$	0.06123	0.05076	0.05999
v_{Zn}	2.1688E-4		1.684E-4
v_{Co}		7.416E-5	1.5224E-5

Also, the amount of Co in the deposited Zn-Co alloy is less than that in pure deposited Co, although the same Co^{2+} concentration in the bath solution.

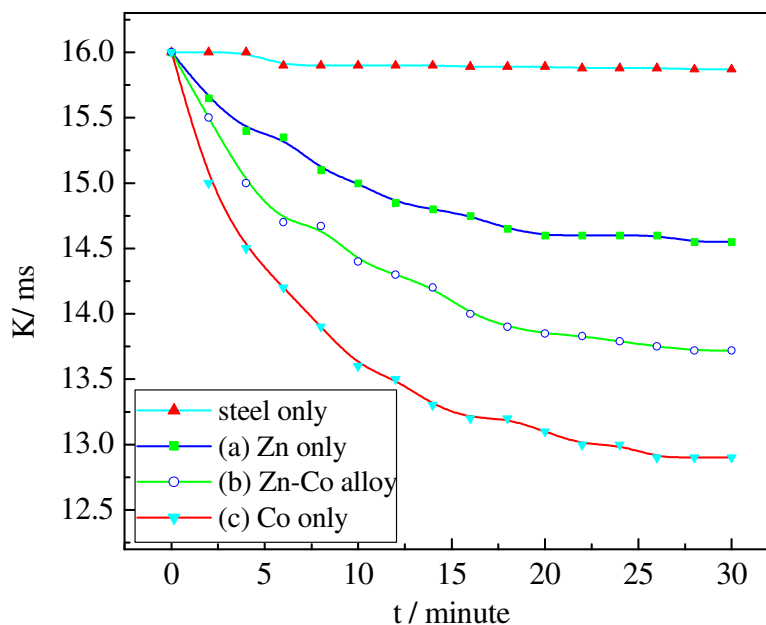


Figure 7. K-t curves for the dissolution of the deposit Zn-Co on steel (12 cm^2), plated from a bath containing 0.20 M ZnSO_4 (a and b), 0.20 M CoSO_4 (b and c), $0.01 \text{ M H}_2\text{SO}_4$, $0.20 \text{ M Na}_2\text{SO}_4$ and $0.20 \text{ M H}_3\text{BO}_3$ at 10 mA cm^{-2} for 10 minutes at 30.0°C , in 100 cm^3 0.20 M HCl at 30.0°C .

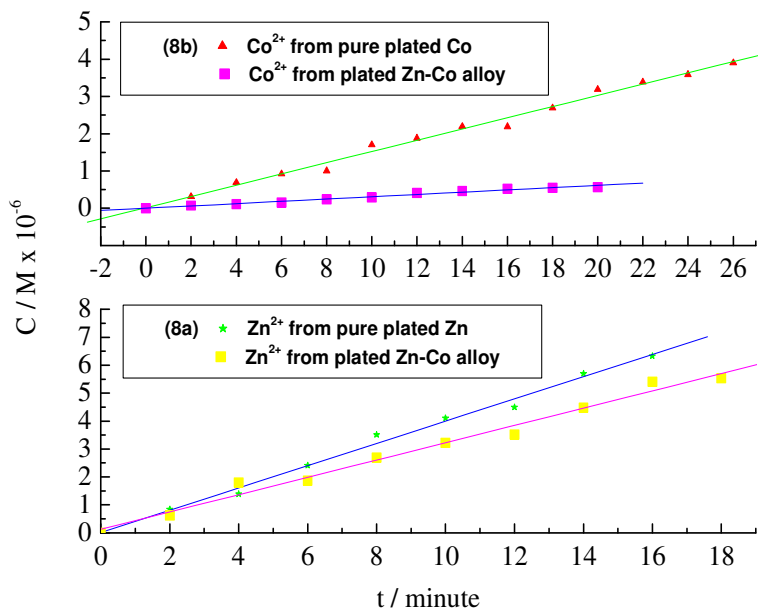


Figure 8. C-t curves for the dissolution of the deposit pure Zn and Co and Zn-Co (8a for Zn) and (8b for Co) on steel (12 cm^2), plated from a bath containing 0.20 M ZnSO_4 , 0.20 M CoSO_4 , $0.01 \text{ M H}_2\text{SO}_4$, $0.20 \text{ M Na}_2\text{SO}_4$ and $0.20 \text{ M H}_3\text{BO}_3$ at 10 mA cm^{-2} for 10 minutes at 30.0°C , in 100 cm^3 0.20 M HCl at 30.0°C .

Figure 8 represented results of the variation of Zn^{2+} (Figure 8a) and Co^{2+} (Figure 8b) concentrations accumulated in HCl during the dissolution of the deposited pure Zn and Co and Zn-Co with time. It was found that Zn^{2+} concentration from Zn-Co dissolution decreased attributable to the presence of Co in the alloy. Also, the dissolution rate v_{Zn} (Table 3) decreased, comparable with pure plated Zn. This is due to the presence of Co in the alloy increases the dissolution resistance of Zn. In the other hand, Co^{2+} concentration from Zn-Co dissolution highly decreased (due to the anomalous codeposition of Co in the alloy). Also, the dissolution rate v_{Co} (Table 3) decreased comparable with pure plated Co. This is may be due to the presence of Zn which is act as a sacrificed metal although the amount of Co is low comparable with pure plated Co.

4. CONCLUSIONS

The present study revealed that the Zn deposition was observed to start at about -1.096 V, which close to Zn-Co codeposition (about -1.06 V). The Co deposition started at about -0.87 V and the deposited layer gradually growth with increase of the negative potential. Also, the polarization curve of the alloy deposition lies between the polarization curves of the separate deposition of Zn and Co. This position suggested that the codeposition enable Zn to deposit at more positive potential and increasing that of Co due to that the Co^{2+} facilitates the Zn deposition.

It is clear that the deposition of Co needs low overpotential to create the initial nucleus and the deposit grow at low potentials. The depositions of Zn take place with higher nucleation overpotential and grow at high potential. The Zn-Co codeposited at moderate overpotential; this due to the deposition of Co is strongly inhibited by the presence of Zn^{2+} , while the deposition of Zn is induced by the presence of Co^{2+} . Also, the plated Zn-Co had the best resistance of the coating tested than plated Zn only. Thus, the improvement achieved in the corrosion resistance of alloy deposits can explained by the presence of Co.

The present work shows that both of the two used methods (stripping and conductance measurements) are satisfactory. The stripping analysis was found more acceptable one for studying the dissolution of Zn-Co alloy due to that analysis detect the very small concentrations of dissolved Zn or Co.

Under the examined conditions, the electrodeposition of the alloy has belonged to the anomalous type and the alloy consisting of the two phases pure Zn and γ - phase.

References

1. I. Brooks and U. Erb, *Scripta Mater.*, 44 (2001) 853.
2. M. M. Abou-Krishna, *J. Appl. Surf. Sci.*, 252 (2005) 1035.
3. M. E. Bahrololoom, D. R. Gabe and G. D. Wilcox, *Trans. IMF*, 82 (2004) 51.
4. D. Carpenter, M. Ashworth and J. Farr, *Trans. IMF*, 81 (2003) 177.
5. S. Rashwan, A. Mohamed, S. Abdel-Wahaab and M. Kamel, *J. Appl. Electrochem.*, 33 (2003) 1035.
6. Jing-Yin Fei and G. D. Wilcox, *Electrochim. Acta*, 50 (2005) 2693.
7. Z. F. Lodhi, J. M. C. Mol, W. J. Hamer, H. A. Terryn and J. H. W. De Wit, *Electrochim. Acta*,

online (2007).

8. G. Roventi, T. Bellezze and R. Fratesi, *Electrochim. Acta*, 51 (2006) 2691.
9. T. E. Sharples, *Prod. Finish.*, 54 (1990) 38.
10. M. M. Abou-Krishna, F. H. Assaf and A. A. Toghan, *J. Solid State Electrochem.* 11 (2007) 244.
11. M. M. Abou-Krishna, A. M. Zaky and A. A. Toghan, *Asian J. of Biochemistry*, 1 (2006) 84.
12. A. M. Alfantazi, J. Page and U. Urb, *J. Appl. Electrochem.* 26 (1996) 1225.
13. L. Anicai, M. Siteavu and E. Grunwald, *Corros. Prevent. Control*, 39 (1992) 89.
14. T. Akiyama and H. Fukushima, *ISIJ Int.*, 32 (1992) 787.
15. A. Brenner, *Electrodeposition of alloys*, Vol. 2, Academic Press, New York, (1963) p. 194.
16. M. J. Nicol and H. I. Philip, *J. Electroanal. Chem.*, 70 (1976) 233.
17. S. Swathirajan, *J. Electrochem. Soc.*, 133 (1986) 671.
18. M. Matlosz, *J. Electrochem. Soc.*, 140 (1993) 2272.
19. Y. Keith Sasaki and B. Jan Talbot, *J. Electrochem. Soc.*, 147 (2000) 189.
20. W. C. Grande and J. B. Talbot, *J. Electrochem. Soc.*, 140 (1993) 675.
21. N. Zech, E. J. Poldlaha and D. Landolt, *J. Electrochem. Soc.*, 146 (1999) 2886.
22. C. Bowden and A. Matthews, *Surface and Coating Technology*, 76 (1995) 508.
23. M. Siluvai Michael, M. Pushpavanam and K. Balakrishnan, *British Corrosion Journal*, 30 (1995) 317.
24. M. Khodari, M. M. Abou-krishna, F. H. Assaf, F. M. El-Cheikh and A. A. Hussien, *Materials Chemistry and Physics*, 71 (2001) 279.
25. F. H. Assaf, M. M. Abou-krishna, M. Khodari, F. M. El-Cheikh and A. A. Hussien, *Materials Chemistry and Physics*, 77 (2002) 192.
26. M. Abou-Krishna and M. J. Jaskula, *Acta Metallurgica Slovaca*, 4 (2001) 9.
27. F. M. El-Cheikh, F. H. Assaf, M. Khodari, A. Gandour and M. M. Abou-krishna, *Bull. Chem. Soc. Jpn.*, 67 (1994) 2286.
28. M. M. Ghoneim, A. M. Hassanein, E. Hammam and A. M. Beltagi, *J Anal Chem.*, 367 (2000) 378.
29. Robert D. Braun, *Introduction to Chemical Analysis*, McGraw-Hill, New York (1983).